PERIODICO di MINERALOGIA
established in 1930

Dipartimento
di Scienze della Terra

Sapienza
Università di Roma

An International Journal of
Mineralogy, Crystallography, Geochemistry,
Ore Deposits, Petrology, Volcanology
and applied topics on Environment, Archaeometry and Cultural Heritage

Post-collisional Plio-Pleistocene Anar-Dehaj adakitic subvolcanic domes in the central volcanic belt of Iran: geochemical characteristics and tectonic implications

Alireza Shaker Ardakani

Department of Mining Engineering, Higher Education Complex of Zarand, Shahid Bahonar University of Kerman, Iran

ARTICLE INFO

Submitted: September 2015
Accepted: August 2016
Available on line: September 2016

* Corresponding author: shaker@uk.ac.ir

DOI: 10.2451/2016PM610

How to cite this article: Shaker Ardakani A. (2016) Period. Mineral. 85, 184-183

ABSTRACT

In the area between Anar and Dehaj, located in the Urumieh-Dokhtar magmatic assemblage (UDMA), there are some Plio-Pleistocenic subvolcanic porphyritic andesitic-dacitic domes. The subvolcanic domes, as a part of Dehaj-Sarduieh belt in Kerman province, show tafoni erosion and magma mingling evidences. Petrographically, the domes are andesite and trachyandesite in composition and are characterized by microlitic-porphyritic, glomeroporphyritic, trachytic and aphanitic textures. Mineralogically, the domes consist of plagioclase, amphibole, clinopyroxene and opaque minerals.
Geochemical studies reveal that Anar-Dehaj subvolcanic domes can be divided two groups, named group 1 and group 2, on the basis of the silica content. Group 1 shows high-K calc-alkaline andesite-trachyandesite composition; whereas group 2 is medium-K calc-alkaline dacite. The absence of a distinct Eu anomaly in all samples suggests contemporaneous crystallization of plagioclase and amphibole, and/or oxidation state of magma. Trace element discrimination diagrams along with chondrite-normalized rare earth element patterns show that the Anar-Dehaj subvolcanic rocks formed in a subduction related environment. Moreover, high Sr/Y and La/Yb ratios along with low Y and HREE contents are consistent with adakitic natures. It is suggested that the Anar-Dehaj subvolcanic domes formed in a post-collisional setting due to slab melting or underplating of basaltic magmas under thick Plio-Pleistocene continental crust.

Keywords: Adakite; Subduction zone; Post-collision; Urumieh-Dokhtar magmatic assemblage; Dehaj-Sarduieh belt; Iran.

INTRODUCTION

The term 'adakite', firstly proposed by Defant and Drummond (1990), is widely used to represent silica-rich, high Sr/Y and La/Yb volcanic and plutonic rocks that form in a variety of tectonic settings (e.g., subduction zones, continental collision zones, and extensional environments) via various petrogenetic processes (Defant and Drummond, 1990; Atherton and Petford, 1993; Xu et al., 2002; Chung et al., 2003; Hou et al., 2004; Wang et al., 2005; Guo et al., 2007; Castillo, 2012; Zheng et al., 2014). Adakites usually form suites of intermediate to felsic rocks whose compositions range from hornblende-andesite to dacite and rhyolite (Defant and Drummond, 1990; Maury et al., 1996; Martin, 1999). Also these rocks show Al_2O_3>15 wt%, MgO<6 wt%, low Y and heavy rare earth element (HREE) contents (Y and Yb<18 and 1.9 ppm, respectively) and high large ion lithophile element (LILE) contents with Sr>400 ppm (Defant et al., 1992).

Martin and Moyen (2003) classified adakites to two main compositional groups based on the silica contents: high-SiO_2 adakites (HSA; SiO_2>60 wt%) and low-SiO_2 adakites (LSA; SiO_2<60 wt%). The difference pointed out between HSA and LSA is not simply a subtle difference in mineralogy or in chemistry or an artifact of classification. Rather, it reflects a fundamental difference in petrogenesis, and specifically in different sources. The primary source of HSA is subducted oceanic crust, but the resulting melts also interact with peridotite during their ascent through the mantle wedge. LSA are generated in two distinct episodes; complete consumption of slab-melt during melt-peridotite interaction, followed by melting of the metasomatised peridotite source (Martin et al., 2005).

TECTONIC HISTORY OF THE REGION

The geological and tectonic history of Iran is linked to the evolution of Tethyan Ocean. The Central Iranian microcontinent was detached from Gondwanaland during Permian to Early Triassic time and subsequently attached to Eurasia along the Alborz and Kopeh-Dagh sutures during Triassic closure of the Paleo-Tethys Ocean (Stocklin, 1968; Falcon, 1974; Stoneley, 1981). As the Paleo-Tethys Ocean was closing, rifting along the present Zagros thrust zone took place on the continental plate. This eventually led to the opening of the Neo-Tethys Ocean (Berberian and Berberian, 1981). The new ocean was expanded during Late Triassic-Early Jurassic, while pelagic marine carbonates were deposited in Zagros orogenic belt. The Zagros orogenic belt of Iran belonging to the extensive Alpine-Himalayan orogenic system, formed as a result of the separation of Arabia from Africa and its subsequent collision with Eurasia. Structurally, the Zagros orogenic belt consists of three parallel NW-SE trending units (Figure 1): 1. The Zagros fold-thrust belt (ZFTB) is bounded to the northeast by the Main Zagros Reverse fault and is proposed to be the suture zone between the Arabian plate and Eurasia. The ZFTB contains a thick and almost continuous sequence of shelf sediments deposited on the 1-2-km-thick Infra-Cambrian Hormoz salt formation. These sediments, of Paleozoic to Late Tertiary age, are believed to be separated from the Precambrian metamorphic basement by the Hormoz salt layer (Alavi, 1994; Agard et al., 2005). 2. The Sanandaj-Sirjan zone (SSZ; Stocklin, 1968) is composed of Jurassic interbedded phyllites and meta-volcanic rocks showing moderate metamorphic imprint except close to large scale Mesozoic calc-alkaline plutons where the regional metamorphism is superimposed by metamorphic contact aureoles. These metamorphic rocks are unconformably overlain by the Barremo-Aptian Orbitolina limestones, typical of Central Iran sedimentation (Stocklin, 1968). During most of the second half of the Mesozoic, the SSZ represented an active Andean-like margin whose calc-alkaline magmatic activity progressively shifted northward (Berberian and King, 1981; Sengor, 1990).

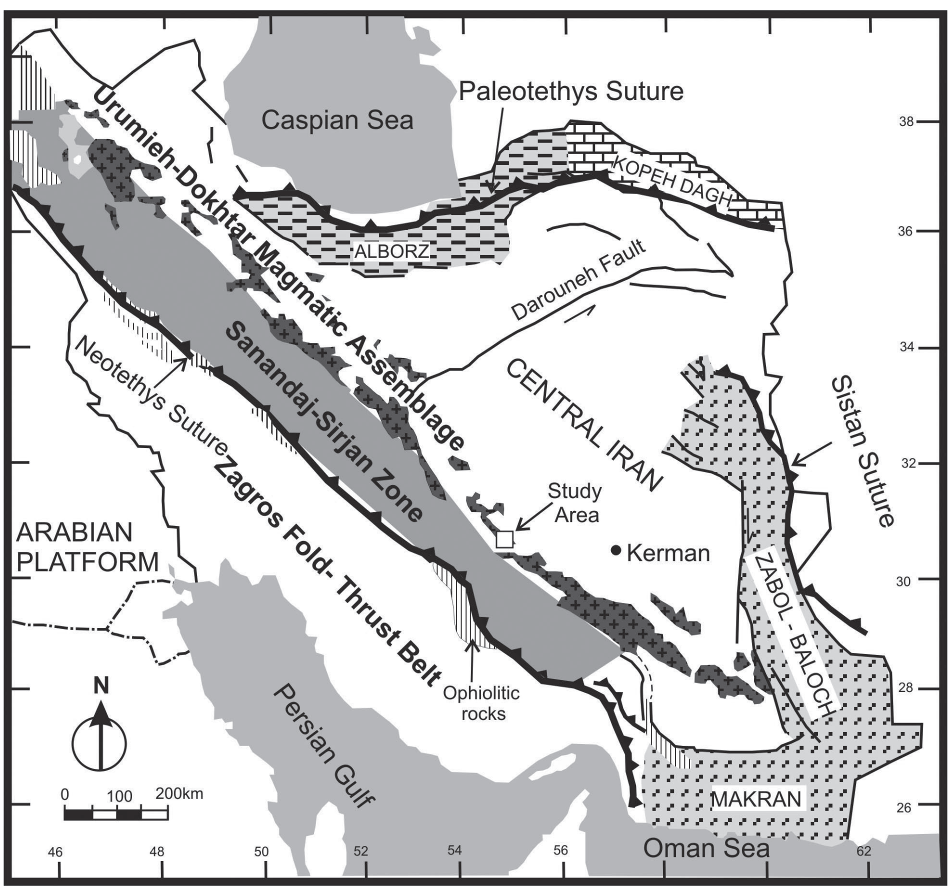

Figure 1. Simplified geological map of Iran illustrating major lithotectonic units in the Zagros orogenic belt and the studied area (after Berberian and King, 1981; Besse et al., 1998; Ghasemi and Talbot, 2006).

3. The Urumieh-Dokhtar volcanic zone of Schroder (1944) or the Urumieh-Dokhtar magmatic assemblage (UDMA) of Alavi (2004) is a 150 km wide igneous complex. This has been interpreted to be a subduction related Andean-type magmatic arc that has been active from the Late Jurassic to the present (Berberian and King, 1981; Berberian et al., 1982). The UDMA is composed of voluminous tholeiitic, calcalkaline, and K-rich alkaline intrusive and extrusive rocks (with associated pyroclastic and volcanoclastic successions) along the active margin of the Iranian plates. The oldest rocks in the UDMA are calc-alkaline intrusive rocks, which cut across Upper Jurassic formations and are overlain unconformably by Lower Cretaceous fossiliferous limestone. The youngest rocks in the UDMA consist of lava flows and pyroclastics that belong to Pliocene to Quaternary volcanic cones of alkaline and calc-alkaline composition (Berberian and Berberian, 1981). The Plio-Quaternary volcanism was suggested to have formed as a result of modification of geothermal gradients due to uplift and erosion, or strike-slip shearing motion created by sideways movement of fault blocks due to the continued convergence of Arabia and Eurasia, or to the existence of large strike-slip faults which could develop a region of relative tension at their ends (Berberian and King, 1981). The southeast segment of the UDMA in the Kerman province was named Dehaj-Sarduieh belt by Dimitrijevic (1973).

The final closure of Neo-Tethys and collision between Arabian and Central Iranian plates took place before or during Late Miocene (Berberian and Berberian, 1981; Berberian et al., 1982; Dargahi, 2007). The collision has been purely continental for the past 5 Ma (Stoneley, 1981; McQuarrie et al., 2003; Agard et al., 2005). The convergence velocity of Arabia with respect to Eurasia is approximately 22±2 mm yr^{-1} in the direction N8±°5E (Vernant, 2004), which has been accommodated by crustal shortening, folding and thrusting deformation in the Zagros, Alborz and Kopeh-Dagh regions and also by lateral displacements of Central Iran blocks along major strike-slip faults (Lensch, 1984). After collision in Late Miocene and as a result of shortening and thickening, volcanic activity continued well into Pleistocene in some parts of UDMA (e.g., basaltic lava flows in Bijar and Shahre-Babak regions), leading to formation of alkaline, calc-alkaline volcanic and subvolcanic rocks.

FIELD GEOLOGY

The Studied area lies in SE of Anar to NW of Dehaj, 180 km northwest of Kerman, in southeastern part of the Urumieh-Dokhtar Magmatic Assemblage (UDMA) of Iran. There are numerous Plio-Pleistocene subvolcanic domes in the area (Figure 2), which are intruded into the volcano-sedimentary rocks of Dehaj-Sarduieh belt in Kerman region (Dimitrijevic, 1973).

The subvolcanic domes show low to medium relief with dacitic-andesitic composition and porphyritic texture.

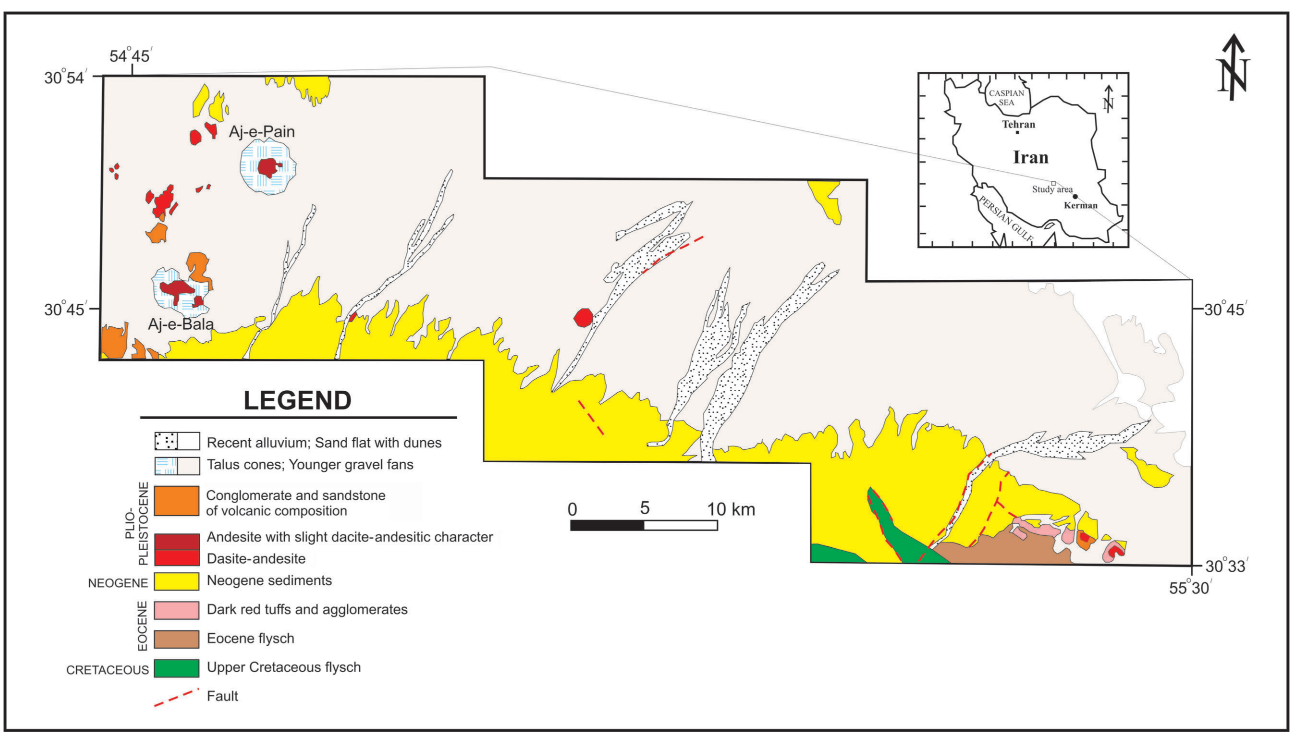

Figure 2. Geological map of the Anar-Dehaj region (modified from Dimitrijevic, 1973).

Plagioclase and amphibole are mainly phenocrysts. The subvolcanic domes exhibit different types of tafoni and exfoliation weathering with mafic banded layers between felsic parts as a sign of magma mingling evidences (Figure 3). The size of weathering pits ranges from 1 cm to 0.5 m in diameter. The pits are oval, more or less spherical, ellipsoidal, and others have irregular forms. Younger phases of this volcanism are represented by the porphyritic andesites of Aj-e-Pain and Aj-e-Bala which consist of plagioclase phenocrysts, basaltic hornblende, variable amounts of biotite, and subordinate crystals of pyroxene and quartz.

ANALYTICAL METHOD

One hundred and fifty rock samples were collected from the subvolcanic domes in the studied area based on 1:100000 geological maps (Dehaj and Anar) and Satellite images. The mineralogy and textures of 53 thin sections were studied with a polarizing microscope. Based on microscope studies, 15 of the freshest and most representative rock samples were selected for sending to ALS Chemex Laboratories, Vancouver, Canada for whole-rock major and trace element analyses. The whole-rock geochemistry of major oxides was determined by X-ray Fluorescence Spectroscopy (XRF). A calcined or ignited sample (0.9 g) was added to 9 g of Lithium Borate Flux (50%-50% $Li_2B_4O_7$-$LiBO_2$), mixed well and fused in an auto fluxer between 1050-1100 °C. A flat molten glass disc was prepared from the resulting melt. This disc was then analysed by X-ray fluorescence spectrometry. For minor and trace elements, including the rare earth element (REE), a prepared sample (0.2 g) was added to lithium metaborate flux (0.9 g), mixed well and fused in a furnace at 1000 °C. The resulting melt was then cooled and dissolved in 100 mL of 4% HNO_3/2% HCl_3 solution. This solution was then analyzed by inductively coupled plasma-mass spectrometry (ICP-MS).

PETROGRAPHY

Petrographically, the Anar-Dehaj lavas are andesite and trachyandesite in composition and they are generally highly microlitic porphyric with a phenocryt content up to 45-50 vol.% consisting mainly of plagioclase, amphibole, clinopyroxene and opaque minerals (Figure 4). Lavas are

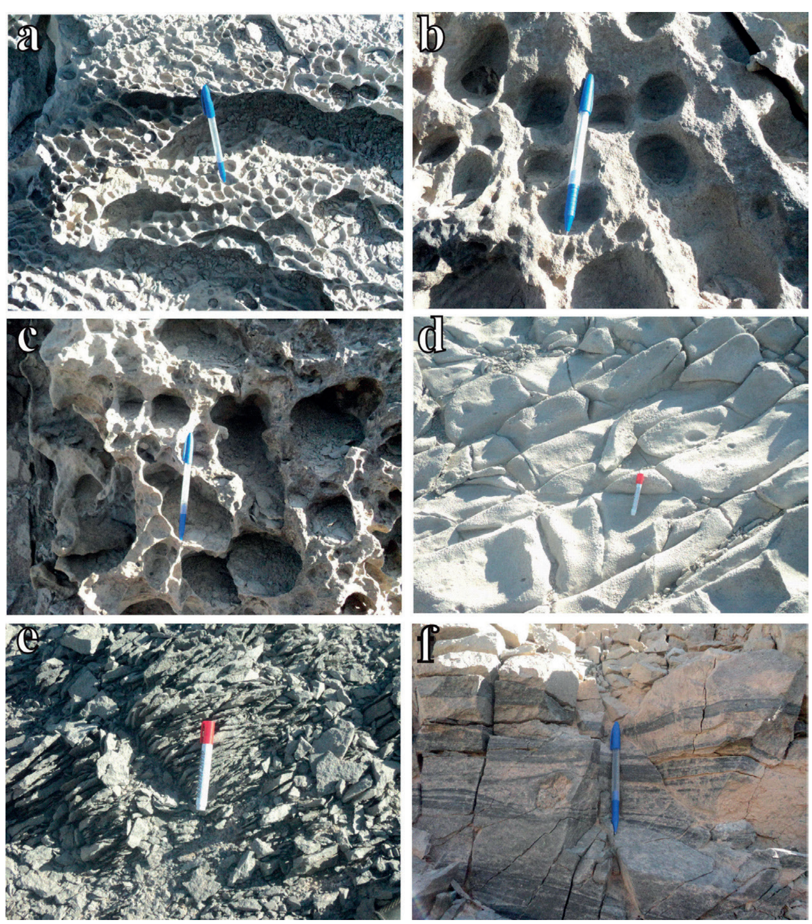

Figure 3. Field views from the Anar-Dehaj subvolcanic domes: (a,b,c and d) different types of tafoni forms; (e) exfoliation weathering; (f) magma mingling structure.

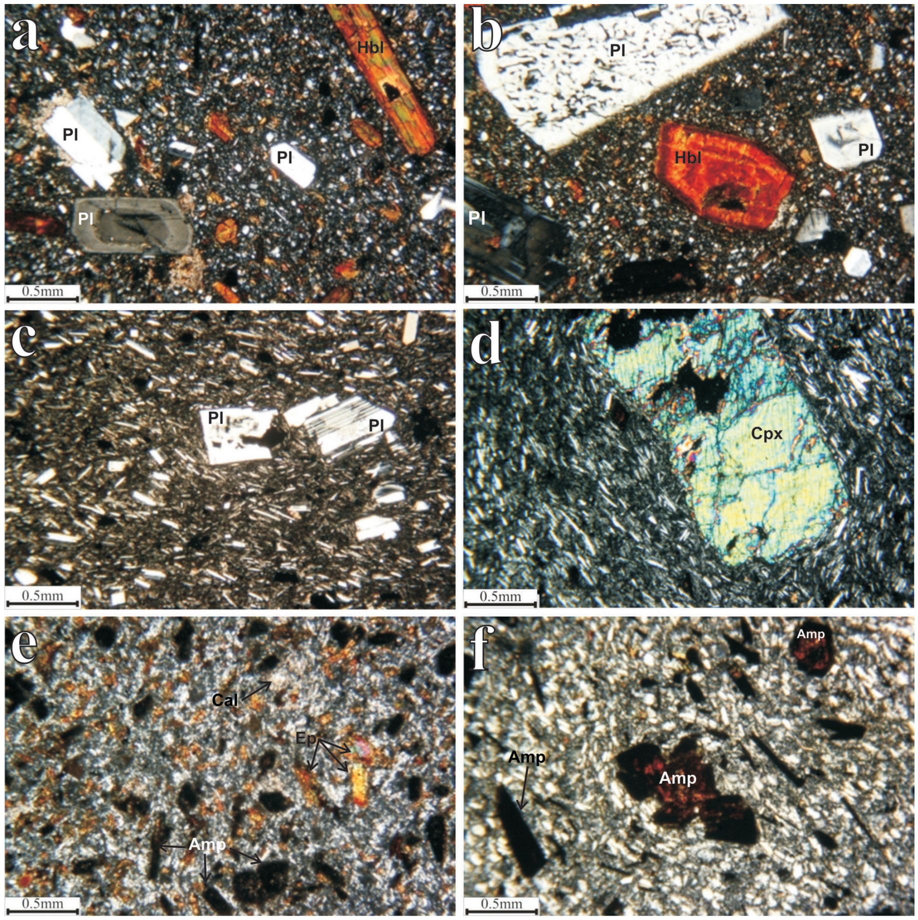

Figure 4. Photomicrographs of andesitic subvolcanic rocks from the studied area: (a) zoned plagioclase (Pl) and hornblende (Hbl) phenocrysts with porphyritic texture; (b) sieved plagioclase with clear rim together zoned hornblende phenocryst; (c) resorbed plagioclase phenocryst; (d) clinopyroxene (Cpx) phenocryst surrounded by plagioclase microlites, which shows microlitic porphyric and trachitic textures; (e) opacitizied amphiboles (Amp) and groundmass consisting of plagioclase, epidote (Ep) and calcite (Cal); (f) partially to completely opacitizied amphiboles, which show glomeroporphyritic texture.

poorly aphanitic and show glomeroporphyritic, hyalo-microlitic porphyric and trachitic textures. Plagioclase is the most abundant mineral which occurs as large (up to 2 mm) euhedral to subhedral phenocrysts as isolated phenocrysts or glomerocrysts and as equant microphenocrysts (100-200 µm in diameter) and lath-shaped microlites (<100 µm) in the groundmass. The plagioclase phenocrysts display sieve texture, resorption and oscillatory zoning as marks of disequilibrium during crystallization. Other disequilibrium signs such as glass inclusions with typical 'honeycomb texture' (Kawamoto, 1992) are also observed in the plagioclases. Amphibole occurs as individual subhedral to euhedral phenocrysts (up to 3 mm in diameter). They are only slightly opacitized and also rarely show zoning. Opacitization of amphiboles suggests high P_{H2O} and f_{O2} conditions during the formation of Anar-Dehaj subvolcanic domes. Clinopyroxene occurs as isolated euhedral to subhedral phenocrysts (up to 2 mm in diameter). Epidote, calcite, chlorite and iron oxides occur as secondary minerals.

GEOCHEMISTRY

Based on geochemical analyses (Table 1), Anar-Dehaj subvolcanic samples can be divided in two groups with low and high silica contents (named in all diagrams as group 1 and group 2, respectively). In Harker diagrams, MgO, Fe_2O_3, TiO_2 and P_2O_5 all have a negative correlation with SiO_2 (Figure 5). Also, the samples record Al_2O_3 contents greater than ~15 wt%. On the Nb/Y vs. Zr/TiO_2 (Winchester and Floyd, 1977; Figure 6a) and Na_2O+K_2O vs. SiO_2 (Irvine and Baragar, 1971; Figure 6b) diagrams the Anar-Dehaj subvolcanics plot mainly in the trachyandesite-rhyodacite/dacite and sub-alkaline fields, respectively. The Anar-Dehaj subvolcanic samples define a typical calcalkaline trend on the AFM diagram (Figure 7a), although on K_2O vs. SiO_2 diagram, some tendency

Table 1. Major and trace element analyses of the Anar-Dehaj rocks.

Sample	A-5	A-16	A-32	A-38	B-4	B-14	D-19	D-25	E-5	F-1	F-5	F-6
Major elements (wt%)												
SiO_2	60.20	61.80	61.60	62.00	55.90	57.60	56.50	54.4	64.40	64.80	64.00	65.00
Al_2O_3	15.70	15.05	15.40	15.80	14.80	14.97	14.83	15.50	16.70	16.25	16.20	16.40
FeO_T	4.88	4.54	5.21	4.38	5.92	5.53	6.06	6.02	3.54	3.33	3.41	3.50
CaO	5.56	4.90	5.69	4.80	7.91	7.44	7.47	7.56	4.27	4.50	4.91	4.40
MgO	2.01	1.77	2.80	1.42	3.49	3.32	4.46	3.70	0.85	1.24	1.16	1.04
Na_2O	4.47	5.30	4.33	4.64	4.01	3.78	4.23	4.45	5.10	5.16	5.00	5.08
K_2O	3.55	2.63	3.59	3.73	2.77	2.99	2.47	2.46	1.88	1.48	1.76	1.87
TiO_2	0.68	0.64	0.72	0.58	0.84	0.79	0.92	0.97	0.45	0.44	0.42	0.43
MnO	0.12	0.10	0.12	0.12	0.10	0.09	0.08	0.08	0.04	0.04	0.04	0.05
P_2O_5	0.40	0.34	0.39	0.32	0.43	0.35	0.46	0.51	0.24	0.18	0.20	0.19
LOI	0.89	2.58	0.39	0.30	1.89	1.96	1.59	2.68	1.37	1.58	1.89	0.29
Total	98.46	99.75	100.24	98.09	98.06	98.82	99.07	98.33	98.83	99.00	98.99	98.25
Trace elements (ppm)												
V	175	132	176	97	179	140	103	147	68	60	49	102
Cr	10	10	20	10	40	40	180	60	10	10	20	10
Co	13.2	11.9	16.1	8.8	19.5	18.6	23.4	20.3	7.7	7.3	7.3	7.7
Ni	8	6	13	<5	16	15	103	46	7	8	8	8
Ga	21.1	21.2	21	20	20.7	19.5	19.1	20.2	22.7	20.7	20.5	20.7
Rb	76.3	81.6	78.8	76.9	65.9	65.6	47.3	59.0	29.5	28.4	27.6	32.3
Sr	1480	1760	1355	1345	1440	1385	1100	1320	996	787	860	814
Y	16.2	15.3	15.5	14.2	16.8	15.4	15.9	17.4	7.9	7.2	7.7	8.5
Zr	167	166	155	160	138	133	176	178	137	140	129	131
Nb	14.0	14.4	13.4	14.1	12.4	10.9	11.7	13.1	4.9	4.1	4.5	4.7
Pb	53	24	22	20	18	17	12	12	10	10	10	10
Cs	1.55	2.47	1.61	1.53	2.04	0.95	1.12	1.68	0.73	0.65	0.48	0.96
Ba	971	1000	960	935	879	827	856	913	512	489	500	503
Hf	4.8	4.8	4.6	4.4	4.3	4.1	4.6	4.8	3.8	3.7	3.5	3.6
Ta	0.9	0.9	0.9	0.9	0.8	0.7	0.7	0.7	0.3	0.2	0.3	0.3
Th	19.10	18.15	16.45	17.75	13.85	11.90	9.30	10.25	4.00	4.22	4.08	3.91
U	5.18	5.04	4.76	4.11	3.81	3.96	2.36	2.91	1.33	1.25	1.04	1.60
La	55.7	50.7	48.8	50.2	43.5	35.3	46.2	51.3	24.3	22.6	23.2	23
Ce	112.5	102.0	97.8.0	100.0	90.8	74.5	90.6	101.0	47.6	43.1	44.1	44.3
Pr	13.30	12.15	11.95	11.95	10.65	8.80	10.65	11.80	5.48	4.90	5.07	5.16
Nb	14.0	14.4	13.4	14.1	12.4	10.9	11.7	13.1	4.9	4.1	4.5	4.7
Sm	7.89	7.41	7.61	7.03	7.22	6.12	7.38	7.88	3.52	3.17	3.25	3.46
Eu	1.93	1.81	1.87	1.70	1.79	1.53	1.96	2.09	1.03	0.9	0.96	0.98
Gd	6.46	6.01	6.21	5.71	6.09	5.21	6.43	6.94	3.20	2.86	2.93	2.96
Tb	0.71	0.67	0.71	0.62	0.70	0.61	0.72	0.76	0.35	0.34	0.36	0.36
Dy	3.32	3.12	3.28	2.89	3.24	2.9	3.22	3.56	1.66	1.52	1.56	1.71
Ho	0.56	0.56	0.60	0.54	0.61	0.57	0.58	0.64	0.29	0.27	0.28	0.31
Er	1.75	1.60	1.72	1.85	1.73	1.65	1.59	1.81	0.77	0.76	0.74	0.86
Tm	0.23	0.22	0.22	0.21	0.23	0.21	0.20	0.23	0.09	0.10	0.10	0.11
Yb	1.48	1.41	1.44	1.34	1.46	1.37	1.28	1.44	0.60	0.60	0.64	0.68
Lu	0.22	0.21	0.22	0.22	0.23	0.21	0.19	0.22	0.09	0.09	0.09	0.10
$(La/Sm)_{cn}$	4.55	4.41	4.14	4.61	3.88	3.72	4.04	4.20	4.44	4.60	4.60	4.29
$(La/Yb)_{cn}$	26.99	25.79	23.30	26.87	21.37	18.48	25.89	25.55	28.96	27.01	26	24.26
Eu/Eu*	0.826	0.829	0.831	0.831	0.825	0.828	0.870	0.863	0.938	0.913	0.951	0.936

Table 1. ...Continued.

Sample	G-1	G-6	H-1
Major elements (wt%)			
SiO_2	63.80	65.10	66.20
Al_2O_3	15.75	16.25	15.96
FeO_T	3.44	3.22	2.93
CaO	4.55	3.86	3.40
MgO	1.15	1.14	0.94
Na_2O	4.83	5.12	4.84
K_2O	1.68	1.71	2.09
TiO_2	0.41	0.42	0.36
MnO	0.03	0.04	0.03
P_2O_5	0.18	0.19	0.16
LOI	2.49	1.08	1.40
Total	98.31	98.13	98.31
Trace elements (ppm)			
V	58	61	51
Cr	10	10	10
Co	7.0	7.2	5.8
Ni	8	8	7
Ga	20.1	20.8	19.6
Rb	29.7	30.5	42.2
Sr	884	777	673
Y	7.3	7.4	7
Zr	139	140	113
Nb	4.0	4.1	4.6
Pb	10	11	13
Cs	0.75	0.76	1.60
Ba	486	509	571
Hf	3.7	3.8	3.2
Ta	0.2	0.3	0.3
Th	4.21	4.43	5.03
U	1.38	1.28	1.85
La	22.6	23.3	20.7
Ce	42.5	44.2	38
Pr	4.85	5.07	4.23
Nb	4.0	4.1	4.6
Sm	3.24	3.31	2.79
Eu	0.89	0.93	0.83
Gd	2.79	2.87	2.48
Tb	0.31	0.33	0.29
Dy	1.47	1.52	1.35
Ho	0.27	0.27	0.25
Er	0.73	0.76	0.71
Tm	0.09	0.09	0.09
Yb	0.63	0.60	0.57
Lu	0.09	0.09	0.08
$(La/Sm)_{cn}$	4.50	4.54	4.97
$(La/Yb)_{cn}$	25.73	27.85	26.05
Eu/Eu*	0.905	0.922	0.965

toward high-k calc-alkaline trend is obvious (Figure 7b) which may point to the depth of subduction.

The diagram CaO/Al_2O_3 vs. FeO_{tot}/MgO (Figure 8a) is used to evaluate the influence of mineral fractionation. Samples align along one single trend controlled by pyroxene and/or amphibole fractionation. The slight positive correlation between TiO_2 and $MgO/(MgO+FeO_{tot})$ in the Anar-Dehaj subvolcanic samples (Figure 8b) suggests that Fe-Ti oxides crystallize simultaneously with ferro-magnesian minerals.

Chondrite-normalized subvolcanic samples (Figure 9) shows enrichments of light REE (LREE) relative to heavy REE (HREE) with a slightly negative Eu-anomaly (Eu/Eu*=0.825-0.965) and flat HREE trend. Relative to HREE, the samples are enriched in LREE [$(La/Yb)_{cn}$=18.48-28.96)]. The absence of a distinct Eu anomaly indicates that either plagioclase fractionation was not significant (Chen et al., 2012), or the magma was relatively oxidized (Magganas, 2002). In general, group 1 shows higher REE contents than group 2.

The Anar-Dehaj subvolcanic domes display low concentrations of HREE and Y (e.g., Yb=0.57-1.48 ppm; Y=7-17.4 ppm). These characteristics, together with high Sr contents (673-1760 ppm) and Sr/Y ratios (76-121), indicate that the samples can be classified as adakites, according to Defant and Drummond (1990) (Figure 10). Furthermore, in Nb vs. SiO_2 and Sr vs. $(CaO+Na_2O)$ diagrams, the group 1 and 2 plot in the fields of low and high silica adakites, respectively (Figure 11; Martin and Moyen, 2003; Martin et al., 2005).

DISCUSSION

On the Th-Zr-Nb diagram (Wood, 1980), all samples plot in the arc-basalts field (Figure 12). The chondrite-normalized incompatible element patterns of the Anar-Dehaj subvolcanic adakite-like rocks (Figure 13) exhibit considerable enrichment in LILEs and negative Nb, Ta and Ti anomalies, suggesting an affinity with magmas generated in a subduction-related tectonic setting. These characteristics can be addressed to two components due to partial melts of subducted sediment and slab derived fluids which may metasomatize and enrich the source region of subduction related magmas (Elburg et al., 2002; Guo et al., 2005). Slab-derived fluids are characterized by high contents of Ba, Rb, Sr, U, and Pb, whereas partial melts of subducted sediments contain high concentrations of Th and LREE (Hawkesworth et al., 1997; Guo et al., 2005; 2007). The Anar-Dehaj subvolcanic adakite-like rocks exhibit variable Ba concentrations (486-1000 ppm) coupled with a range of Nb/Y ratio between 0.55 to 0.99, consistent with the role of both fluid-induced enrichment and subducted sediment components (Figure 14a). Arc settings in which significant amounts of sediments are subducted typically show Th/Yb ratios≥2 (Woodhead

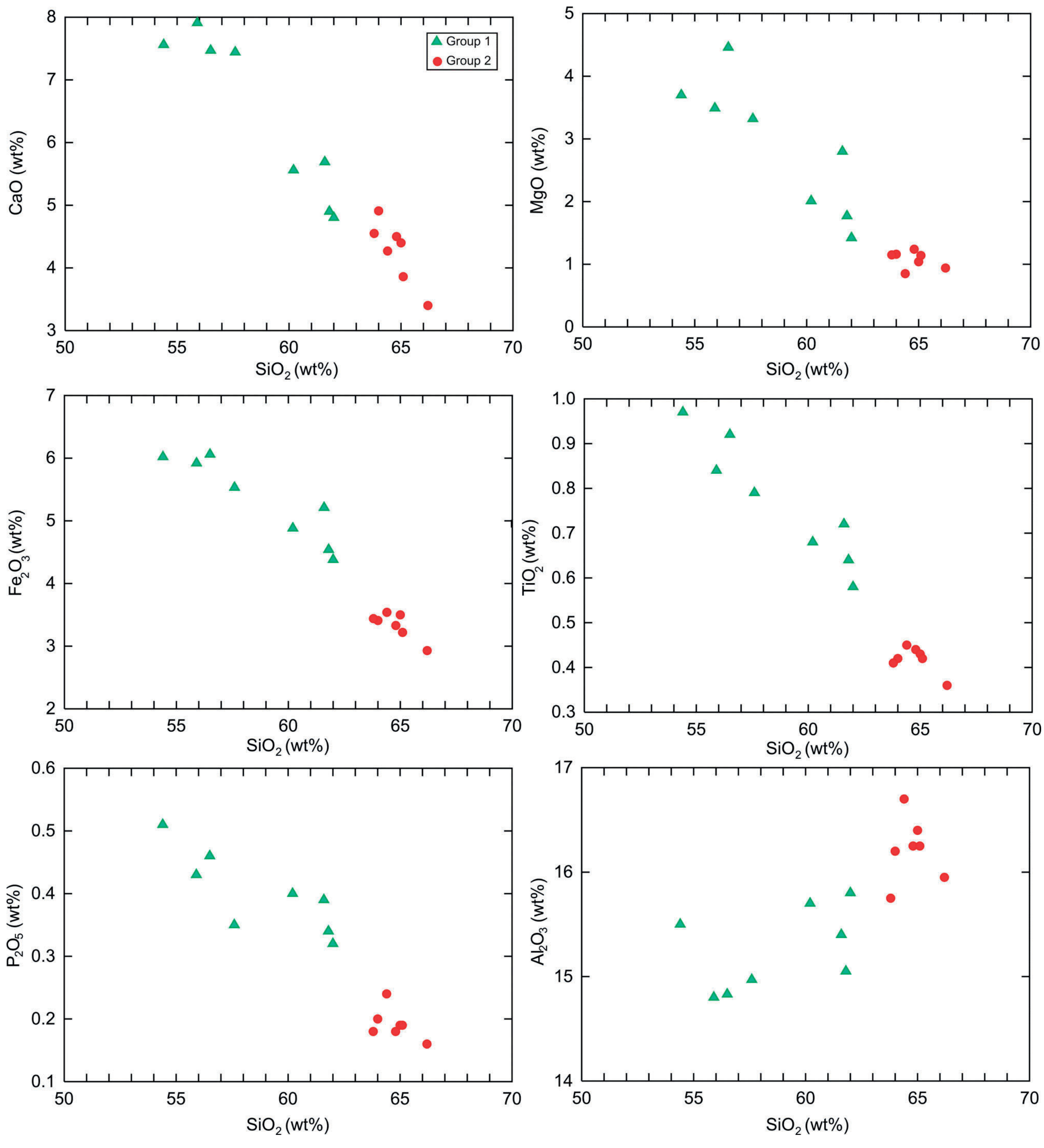

Figure 5. Harker diagrams showing major element variations of the Anar-Dehaj subvolcanic samples.

et al., 2001; Nebel et al., 2007, Zheng et al., 2014).The Anar-Dehaj subvolcanic adakite-like rocks have Th/Yb ratios ranging from 5.75 to 13.25, confirming a significant contribution from due to subduction of sedimentary materials. This is supported by the linear trend of Anar-Dehaj subvolcanic adakite-like rocks depicted on the Th/Yb vs. Th/Sm diagram (Figure 14b). Also, in figure 14b all the samples plot in the post-collisional adakitic field which is in line with the collision time between Arabian and Central Iranian plates and eventually the closure of Neo-Tethys either before or during Late Miocene time (Berberian and Berberian, 1981; Berberian et al., 1982).

The characteristic of low Y and high Sr concentrations of adakite-like rocks (Table 2) such as Anar-Dehaj

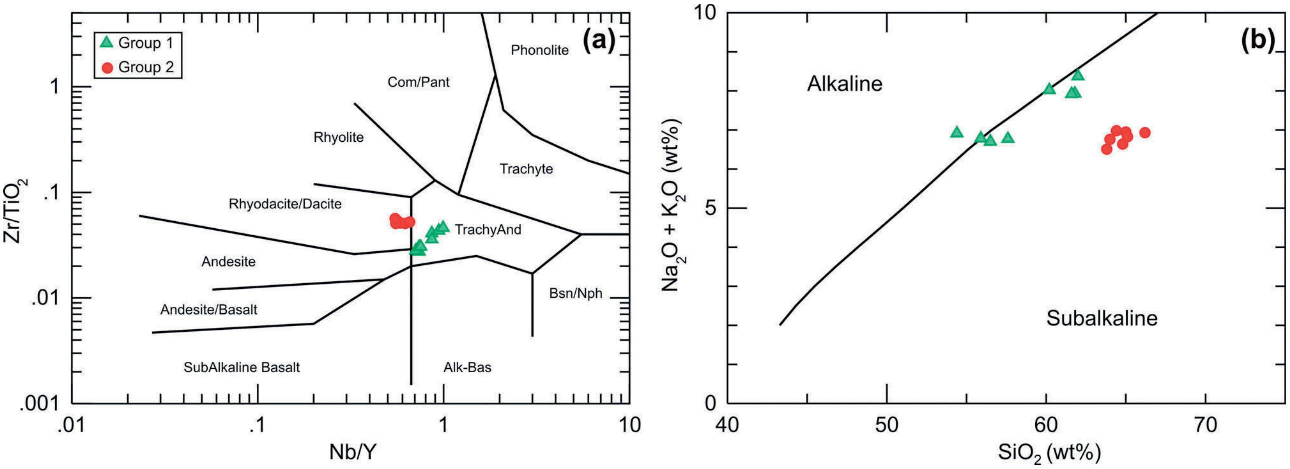

Figure 6. (a) Zr/TiO_2 vs. Nb/Y (Winchester and Floyd, 1977) and (b) Na_2O+K_2O vs. SiO_2 (Irvine and Baragar, 1971) diagrams for the Anar-Dehaj subvolcanic samples.

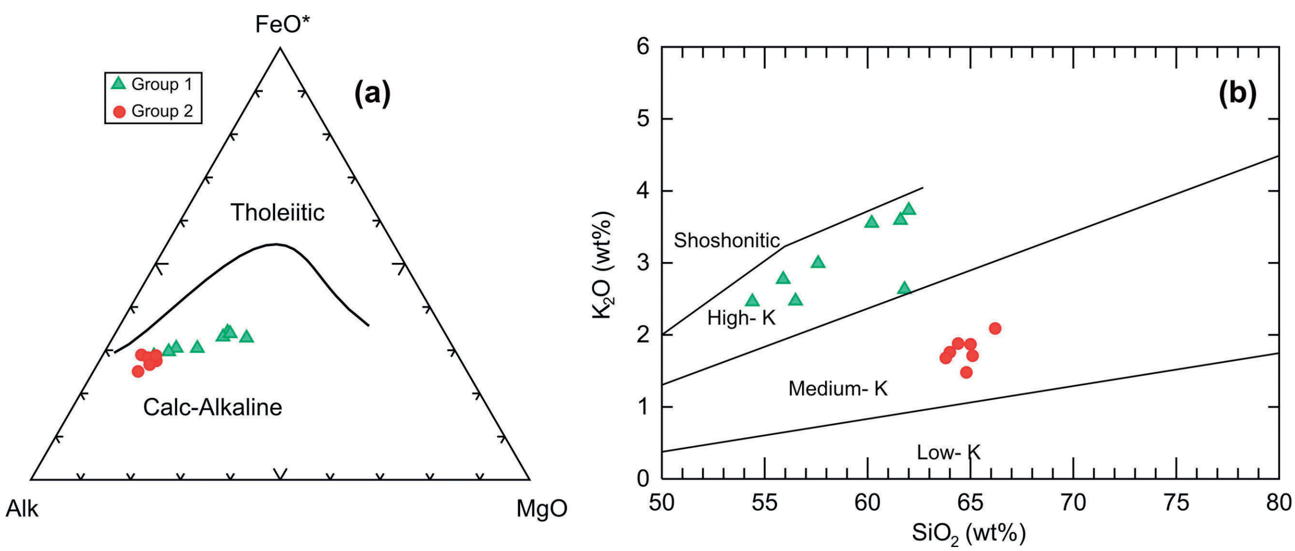

Figure 7. (a) AFM diagram showing chemical trend for the Anar-Dehaj subvolcanic samples, boundary line from Kuno (1968). (b) K_2O vs. SiO_2 classification diagram (after Peccerillo and Taylor, 1976) for the Anar-Dehaj subvolcanic rocks.

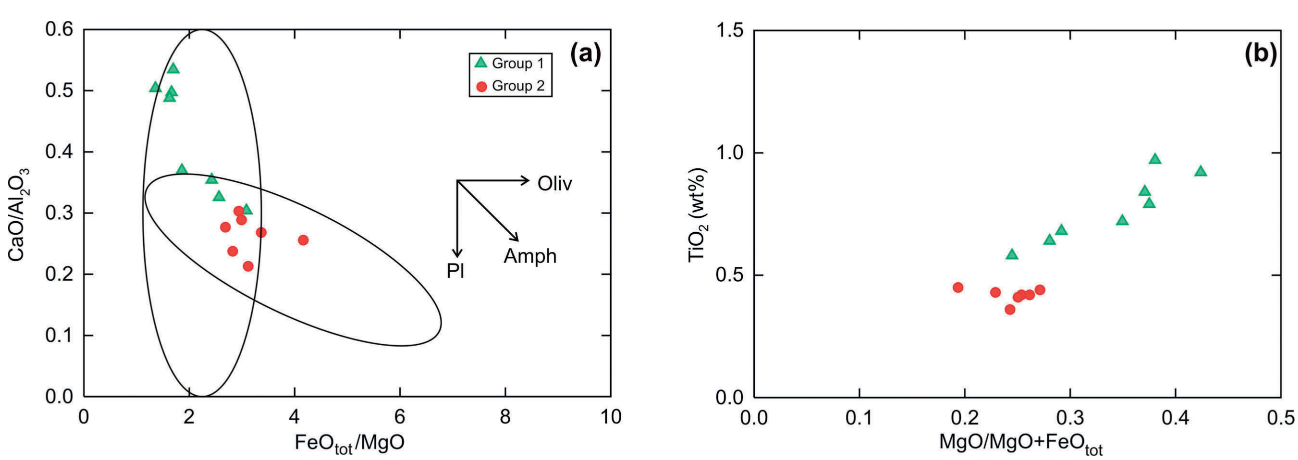

Figure 8. Plot of: (a) CaO/Al_2O_3 vs. FeO_{tot}/MgO; (b) Plot of TiO_2 vs. $MgO/(MgO+FeO_{tot})$.

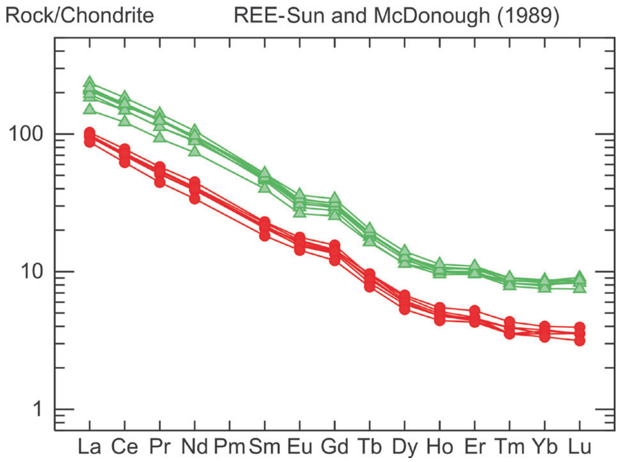

Figure 9. Chondrite-normalized REE patterns for the Anar-Dehaj subvolcanic samples, normalized values from Sun and McDonough (1989).

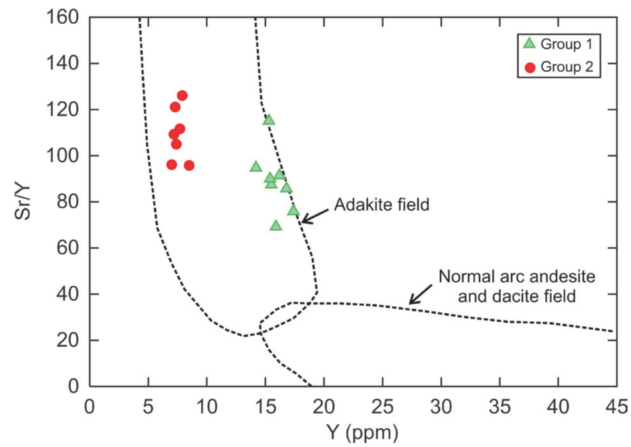

Figure 10. Sr/Y vs. Y discrimination diagram showing data for adakites and normal calc-alkaline rocks (Defant and Drummond, 1990).

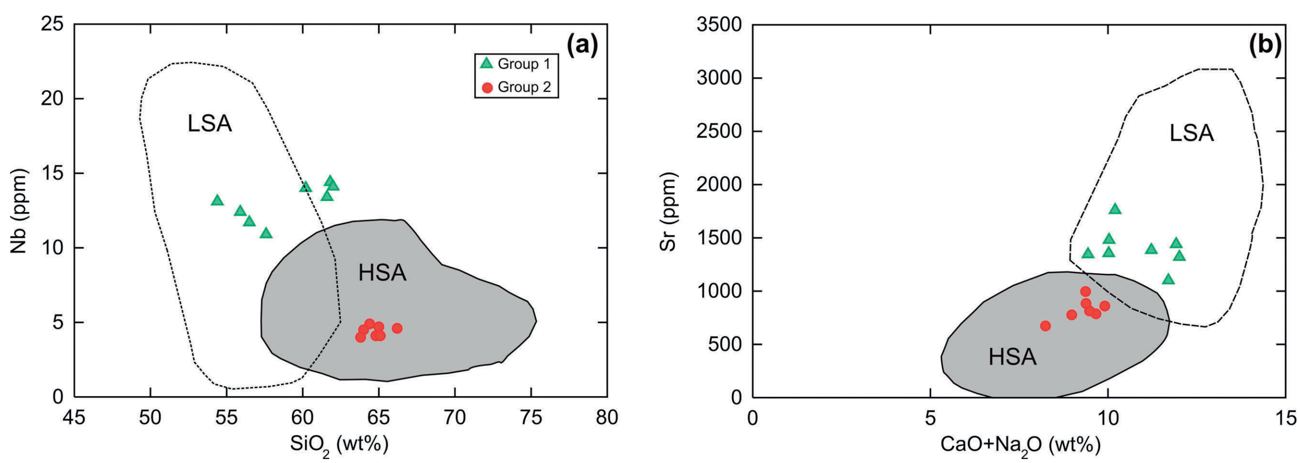

Figure 11. (a) Nb vs. SiO_2, and (b) Sr vs. ($CaO+Na_2O$) diagrams for the Anar-Dehaj subvolcanic samples, boundary line of Martin et al. (2005) (LSA= low silica adakites; HSA=high silica adakites).

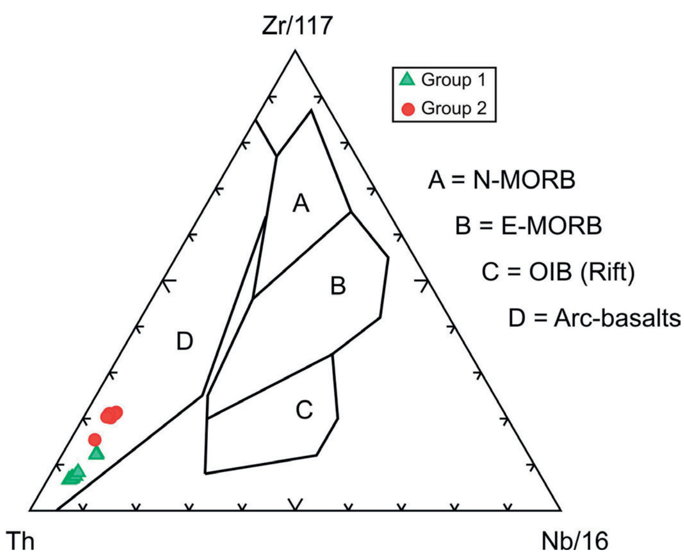

Figure 12. Th-Zr-Nb ternary plot after Wood (1980). All samples plot within the arc-basalt field.

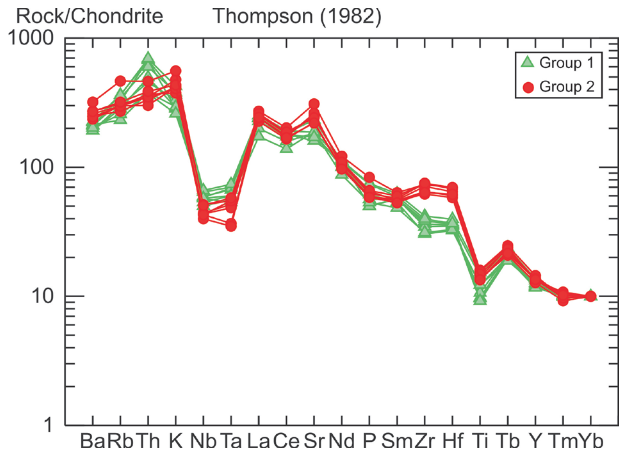

Figure 13. Chondrite-normalized multi-element plots for the the Anar-Dehaj subvolcanic samples, normalized values from Thompson (1982).

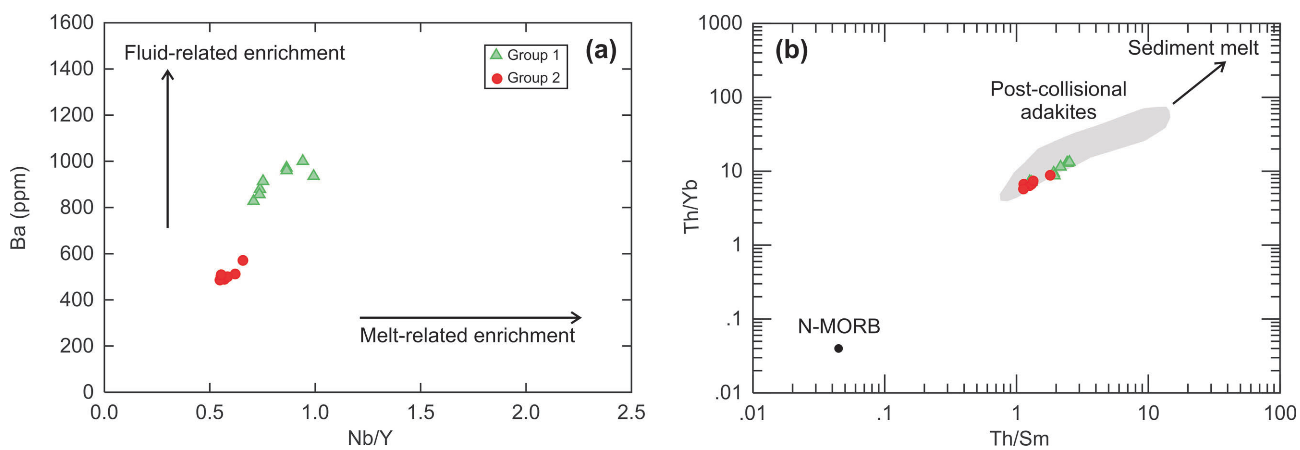

Figure 14. (a) Ba vs. Nb/Y and (b) Th/Yb vs. Th/Sm plots for the Anar-Dehaj subvolcanic rocks. Data for N-MORB from Sun and McDonough (1989).

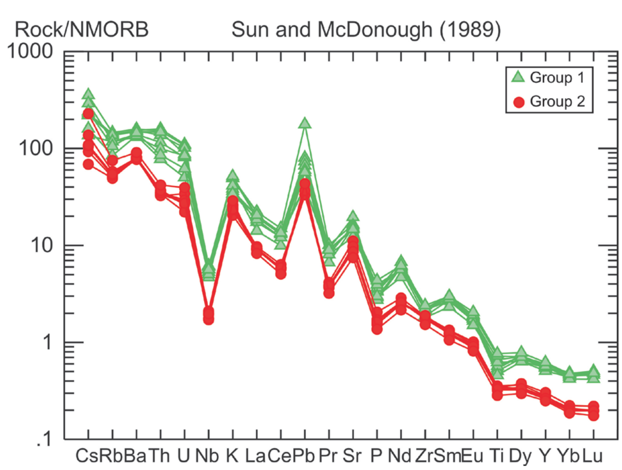

Figure 15. NMORB-normalized multi-element plots for the the Anar-Dehaj subvolcanic samples, normalized values from Sun and McDonough (1989).

Table 2. Main geochemical features of Anar-Dehaj subvolcanic adakite-like samples and their comparison with typical adakites (Defant and Kepezhinskas, 2001; Moyen, 2009).

Adakite characteristics base on Defant and Kepezhinskas (2001)	Adakite characteristics based on Moyen (2009)	Adakite characteristics of the Anar-Dehaj subvolcanic rocks	Possible links to subducted slab melting (Kay, 1978; Defant and Drummond, 1990; Peacock et al., 1994; Rollinson and Martin, 2005)
SiO_2>56 wt%	SiO_2>56 wt%	SiO_2=54.4-66.2%	high-P melting of eclogite/garnet amphibolite
Al_2O_3>15 wt%	Al_2O_3>15 wt%	Al_2O_3=14.8-16.7%	at ~70 wt% SiO_2; high P partial melting of eclogite or amphibolite
MgO<3 wt%	MgO<3 wt%	MgO= 0.85-4.4%	and low Ni and Cr; if primary melt, not derived from a mantle peridotite
Sr>400 ppm	Sr>300 ppm	Sr=673-1760 ppm	melting of plagioclase or absence of plagioclase in the residue
	absence of negative Eu-anomaly	slightly negative Eu-anomaly	either minor plagioclase residue or source basalt depleted in Eu
Y<18ppm	Y<18ppm	Y=7-17.4	indicative of garnet (to a lesser extent, of hornblende or clinopyroxene) as a residual mineral or liquidus phase
Sr/Y>40	Sr/Y>20	Sr/Y=69.18-126.07	higher than that produced by normal crystal fractionation; indicative of garnet and amphibole as a residual mineral or liquidus phase
Yb<1.9 ppm	Yb<1.8 ppm	Yb=0.75-1.48 ppm	meaning low HREE; indicative of garnet as a residual or liquidus phase
La/Yb>20	La/Yb>16	La/Yb=27.5-40.5	LREE enriched relative to HREE; indicative of garnet as a residual or liquidus phase
	Low HFSE (Nb, Ta)	Low HFSE (Nb, Ta)	as in most arc lavas; Ti-bearing mineral or hornblende in the source
	High LREE	High LREE	
	Low HREE	Low HREE	

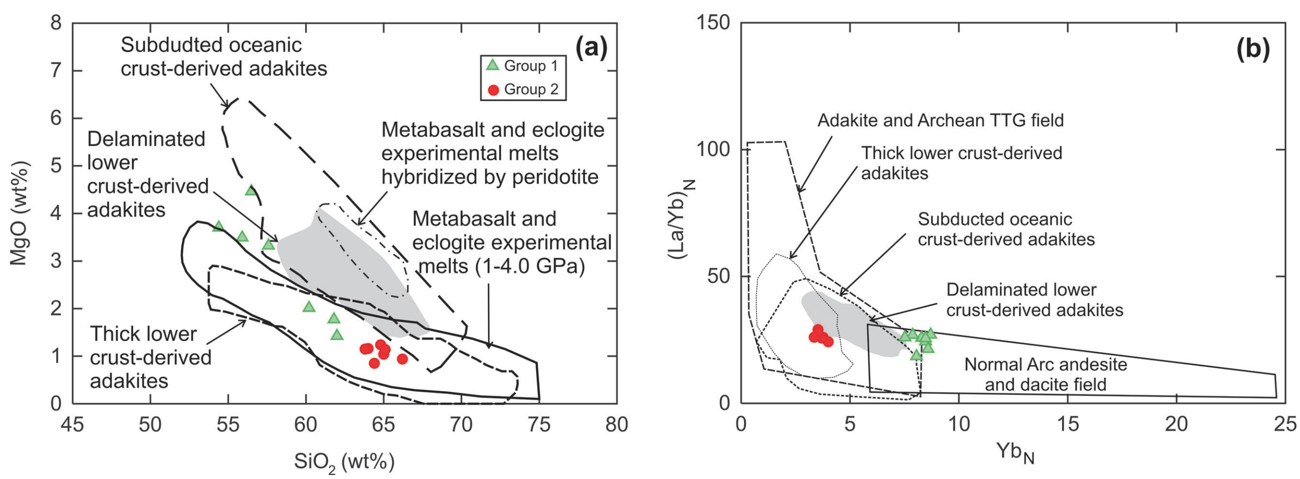

Figure 16. (a) MgO vs. SiO_2 diagram for the subvolcanic rocks from the Anar-Dehaj area. The field of metabasalt and eclogite experimental melts (1-4.0 GPa) is from Rapp et al. (1991; 1999; 2002), Sen and Dunn (1994), Rapp and Watson (1995), Prouteau et al. (1999), Skjerlie and Patiño Douce (2002). The field of metabasalt and eclogite experimental melts hybridized with peridotite is after Rapp et al. (1999). The field of subducted oceanic crust-derived adakites is constructed using data from Defant and Drummond (1990), Kay and Mahlburg-Kay (1993), Drummond et al. (1996), Stern and Kilian (1996), Sajona et al. (2000), Aguillón-Robles et al. (2001), Defant et al. (2002), Calmus et al. (2003), Martin et al. (2005). Data for thick lower crust-derived adakitic rocks are from Atherton and Petford (1993), Muir et al. (1995), Petford and Atherton (1996), Johnson et al. (1997), Xiong et al. (2003). (b) $(La/Yb)_N$ vs. Yb_N plot illustrating the field of adakites and calc-alkaline rocks. Data sources are the same than those from Figure 16a.

subvolcanic samples can be related to alternative magma source processes including melting of an eclogitic or garnet amphibolitic slab and slab melt-mantle interaction (Kay, 1978; Defant & Drummond, 1990; Kay et al., 1993; Kay and Kay, 2002), melting of thickened mafic lower crust (Atherton & Petford, 1993; Kay and Kay, 2002; Chung et al., 2003), and high-pressure fractionation of hydrous magmas with or without melting of lower crust (Castillo et al., 1999; Macpherson et al., 2006; Davidson et al., 2007a; Chiaradia et al., 2009).

The highly enriched N-MORB normalized abundance patterns of trace elements for adakitic andesites-dacites of the Anar-Dehaj subvolcanics suggest the existence of garnet as a residue in the source (Figure 15). The enrichment of Sr and absence of negative Eu anomalies also indicate the absence of plagioclase in the residual source. The Nb and Ti are strongly depleted in the studied samples, pointing out that the source has residual rutile and amphibole and thus, at the time of magma segregation, it was probably hydrous garnet-amphibolite or amphibole-eclogite (Jahangiri, 2007; Ghadami et al., 2008). This garnet-bearing source implies that there are at least two possible mechanisms for the generation of adakitic rocks in Anar-Dehaj subvolcanic domes; partial melting of a thick lower crust and/or melting of subducted oceanic slab.

In Figure 16a most of the subvolcanic samples plot within the fields of "thick lower crust-derived adakite rocks" and "metabasalt and eclogite experimental melts". In Figure 16b, group 1 clearly plots in the overlap of the fields of "island arc" and "adakite and Archean TTG", whereas the group 2 fall within the "subducted oceanic crust derived adakites" field and "thick lower crust derived adakites" field.

CONCLUSION

The Dehaj-Sarduiyeh volcanic belt, which includes the Plio-Pleistocene rocks of the Anar-Dehaj subvolcanic domes, is part of the UDMA. This belt is the subject of considerable controversy concerning the nature and dating of the final closure of the Neotethys Ocean and the Arabian-Central Iranian continental collision process. The existence of the UDMA has been explained by many as the result of a northeast dipping subduction along the Main Zagros reverse fault, at an Andean-type magmatic arc along the active continental margin of Central Iran. Berberian et al. (1982) suggested that the last phase of Andean type magmatic activity in the Urumieh-Dokhtar magmatic zone has taken place during Oligocene-Miocene time which led to the inland migration of the magmatic arc. The significant characteristics of post-colllisional magmatism in the Anar-Dehaj subvolcanic domes also indicate that the final collision between Arabian and Central Iranian plates happened well before Pliocene time.

The Plio-Pleistocene of the post-collisional magmatism in Anar-Dehaj region with adakitic geochemical signatures. indicate the role of slab melting or underplating of basaltic magmas under thick continental crust after the end of subduction. Several authors (e.g., Jahangiri, 2007; Omrani et al., 2008; Ghadami et al., 2008; Shafaii Moghadam et al., 2009) suggest that the temporal and spatial relationship of adakitic rocks in the UDMA may be attributed to slab roll-back and possibly break-off of subducted Neo-Tethyan oceanic lithosphere beneath the Central Iranian continental microplate. Slab break-off may have led to thermal perturbation resulting in melting of detached slab and metasomatism of the mantle in Central Iran during the post-collisional event. This can cause generation of adakitic magmatism such as Anar-Dehaj subvolcanic domes in the UDMA.

ACKNOWLEDGEMENTS
The author would like to thank anonymous reviewers for their critical and constructive comments on the manuscript.

REFERENCES

Agard P., Omrani J., Jolivet L., Mouthereau F. (2005) Convergence history across Zagros (Iran): constraints from collisional and earlier deformation. International Journal of Earth Sciences 94, 401-419.

Aguillón-Robles A., Calmus T., Bellon H., Maury R.C., Cotton J., Bourgois J., Michaud F. (2001) Late Miocene adakites and Nbenriched basalts from Vizcaino Peninsula, Mexico: indicators of East Pacific Rise subduction below southern Baja California. Geology 29, 531-534.

Alavi M. (1994) Tectonics of the Zagros orogenic belt of Iran: new data and interpretations. Tectonophysics 229, 211-238.

Alavi M. (2004) Regional Strational of the Zagros Fold-Thrust Belt of Iran and Its Proforeland Evolution. Amerrican Journal of Science 304, 1-20.

Atherton M.P. and Petford N. (1993) Generation of sodium-rich magmas from newly underplated basaltic crust. Nature 362, 144-146.

Berberian F. and Berberian M. (1981) Tectono-plutonic episodes in Iran. In: Gupta H.K. and Delany F.M. (eds): Zagros, Hindukosh, Himalaya. Geodynamic Evolution. American Geophysical Union, Washigton DC, 5-32.

Berberian F., Muir I. D., Pankhurst R. J. and Berberian M. (1982) Late Cretaceous and Early Miocene Anden-type plutonic activity in northern Makran and Central Iran. Journal of the Geological Society, London, 139, 605-614.

Berberian M. and King G.C.P. (1981) Towards a paleogeography and tectonic evolution of Iran. Canadian Journal of Earth Sciences 18, 210-265.

Besse J., Torcq F., Gallet Y., Ricou L.E., Krystyn L., Saidi A. (1998) Late Permian to Late Triassic palaeomagnetic data from Iran: constraints on the migration of the Iranian block through the Tethyan Ocean and initial destruction of Pangaea. Geophysical Journal International 135, 77-92.

Calmus T., Aguillon Robles A., Maury R.C., Bellon H., Benoit M., Cotton J., Bourgois J., Michaud F. (2003) Spatial and temporal

evolution of basalts and magnesian andesites («bajaites») from Baja California, Mexico: the role of slab melts. Lithos 66, 77-105.
Castillo P.R. (2012) Adakite petrogenesis. Lithos (134-135), 304-316.
Castillo P.R., Janney P.E., Solidum R. (1999) Petrology and geochemistry of Camiguin Island, southern Philippines: insights into the source of adakite and other lavas in a complex arc tectonic setting. Contributions to Mineralogy and Petrology, 134, 33-51.
Chen Y.X., Xia X.H., Song S.G. (2012) Petrogenesis of Aoyougou high-silica adakite in the North Qilian orogen, NW China: Evidence for decompression melting of oceanic slab. Chinese Science Bulletin 57, 2289-2301.
Chiaradia M., Müntener O., Beate B., Fontignie D. (2009) Adakite-like volcanism of Ecuador: lower crust magmatic evolution and recycling. Contributions to Mineralogy and Petrology 158, 563-588.
Chung S.L., Liu D.Y., Ji J.Q., Chu M.F., Lee H.Y., Wen D.J., Lo C.H., Lee T.Y., Qian Q., Zhang Q. (2003) Adakites from continental collision zones: melting of thickened lower crust beneath southern Tibet. Geology 31, 1021-1024.
Dargahi S. (2007) Post-collisional Miocene magmatism in the Sarcheshmeh-Shahrebabak region NW of Kerman: Isotopic study, petrogenetic analysis and geodynamic pattern of granitoid intrusives and the role of adakitic magmatism in development of copper minralization. Ph.D. thesis, Shahid Bahonar University of Kerman, 310 pp.
Davidson J., MacPherson C., Turner S. (2007a) Amphibole control in the differentiation of arc magmas. Geochimica et Cosmochimica Acta 71, A204-A204.
Defant M.J. and Drummond M.S. (1990) Derivation of some modern arc magmas by melting of young subducted lithosphere. Nature 347, 662-665.
Defant M.J., Jackson T.E., Drummond M.S., De Boer J.Z., Bellon H., Feigenson M.D., Maury R.C., Stewart R.H. (1992) The geochemistry of young volcanism throughout western Panama and southeastern Costa Rica: an overview. Journal of the Geological Society 149, 569-579.
Defant M.J., Xu J.F., Kepezhinskas P., Wang Q., Zhang Q., Xiao L. (2002) Adakites: some variations on a theme. Acta Petrologica Sinica 18, 129-142.
Defant M.J. and Kepezhinskas P. (2001) Evidence suggests slab melting in arc magmas. EOS Trans., 20, American Geophysical Union, Washington DC, 82, 67-69.
Dimitrijevic M.D. (1973) Geology of Kerman region. Geological Survey of Iran. Report No, Yu/52, Tehran, 334 pp.
Drummond M.S., Defant M.J., Kepezhinkas P.K. (1996) The petrogenesis of slab derived trondhjemite-tonalite-dacite/ adakite magmas. Transaction of the Royal Society of Edinburgh, Earth Sciences 87, 205-216.
Elburg M.A., Van Bergen M., Hoogewerff J., Foden J., Vroon P., Zulkarnain I., Nasution A. (2002) Geochemical trends across an arc-continent collision zone: magma sources and slab-wedge transfer processes below the Pantar Strait volcanoes, Indonesia. Geochimica et Cosmochimica Acta 66, 2771-2789.
Falcon N. (1974) Southern Iran-Zagros Mountains, in Spencer, A.M., editor, Mesozoic-Cenozoic orogenic belts. Geological Society, London, Special Publications 4, 199-211.
Ghadami G., Shahre Babaki A.M., Mortazavi M. (2008) Post-Collisional Plio-Pleistocene Adakitic Volcanism in Centeral Iranian Volcanic Belt: Geochemical and Geodynamic Implications. Journal of Sciences, Islamic Republic of Iran 19, 223-235.
Ghasemi A. and Talbot C.J. (2006) A new tectonic for the Sanandaj-Sirjan Zone (Iran). Journal of Asian Earth Sciences 26, 683-693.
Guo Z.F., Wilson M., Liu J.Q. (2007) Post-collisional adakites in south Tibet: products of partial melting of subduction-modified lower crust. Lithos 96, 205-224.
Guo Z. Hertogen J., Liu J., Pasteels P., Boven A., Punzalan L., He H., Luo X., Zhang W. (2005) Potassic magmatism in western Sichun and Yunnan provinces, SE Tibet, China: petrological and geochemical constraints on petrogenesis. Journal of Petrology 46, 33-78.
Hawkesworth C., Turner S., Peate D., McDermott F., van Calsteren P. (1997) Elemental U and Th variations in island arc rocks: implications for U-series isotopes. Chemical Geology 139, 207-221.
Hou Z.Q., Gao Y.F., Qu X.M., Rui Z.Y., Mo X.X. (2004) Origin of adakitic intrusives generated during mid-Miocene east-west extension in southern Tibet. Earth and Planetary Science Letters 220, 139-155.
Irvine T.N. and Baragar W.R.A. (1971) A guide to the chemical classification of the common volcanic rocks. Earth and Planetary Science Letters 8, 523-548.
Jahangiri A. (2007) Post-collisional Miocene adakitic volcanism in NW Iran: Geochemical and geodynamic implications. Journal of Asian Earth Sciences 30, 433-447.
Johnson K., Barnes C.G., Miller C.A. (1997) Petrology, geochemistry, and genesis of high-Al tonalite and trondhjemites of the Cornucopia stock, Blue Mountains, Northeastern Oregon. Journal of Petrology 38, 1585-1611.
Kawamoto T. (1992) Dusty and honeycomb plagioclase: Indicators of processes in the Uchino stratified magma chamber, Izu Peninsula, Japan. Journal of Volcanology and Geothermal Research 49, 191-208.
Kay R.W. (1978) Aleutian magnesian andesites: melts from subducted Pacific Ocean crust. Journal of Volcanology and Geothermal Research 4, 117-132.
Kay R.W. and Kay S.M. (2002)Andean adakites, three ways to make them. Acta Petrologica Sinica 18, 303-311.
Kay R.W. and Mahlburg-Kay S. (1993) Delamination and delamination magmatism. Tectonophysics 219, 177-189.
Kay S.M., Romas V.A., Marquez M. (1993) Evidence in Cerro Pampa volcanic rocks for slab-melting prior to ridge-trench collision in southern south America. Geology 101, 703-714.
Kuno H. (1968) Differentiation of basalt magmas. In: H.H. Hess and A. Poldervaart (Editors), Basaltes: The Poldervaart treatise on rocks of basaltic composition, Vol. 2. Interscience, New York , 623-688 pp.
Lensch G. (1984) Plate tectonic, orogeny and mineralization in the Iranian fold belts. Neues Jahrbuch für Geologie und Paläontologie, Abhandlungen 168, 145-568.
Macpherson C.G., Dreher S.T., Thirlwall M.F. (2006) Adakites without slab melting: high pressure differentiation of island arc magma, Mindanao, the Philippines. Earth and Planetary Science Letters 243, 581-593.
Magganas A.C. (2002) Constraints on the petrogenesis of Evros ophiolite extrusives, NE Greece. Lithos 65, 165-182.

Martin H. (1999) The adakitic magmas: modern analogues of Archean granitoids. Lithos 46, 411-429.

Martin H. and Moyen J.F. (2003) Secular changes in TTG composition: comparison with modern adakites. EGS-AGU-EUG joint meeting. Nice, April, VGP7-1FR2O-001.

Martin H., Smithies R.H., Rapp R., Moyen J.F., Champion D. (2005) An overview of adakite, tonalite-trondhjemite-granodiorite (TTG), and sanukitoid: relationships and some implications for crustal evolution. Lithos 79, 1-24.

Maury R.C., Sajona F.G., Pubellier M., Bellon H., Defant M.J. (1996) Fusion de la croûte océanique dans les zones de subduction/collision récentes: l'exemple de Mindanao (Philippines). Bulletin de la Société Géologique de France 167, 579-595.

McQuarrie N., Stock J.M., Verdel C.,Wernicke B.P. (2003) Cenozoic evolution of Neotethys and implications for the causes of plate motions. Geophysical Research Letters 30, 2036.

Moyen J.F. (2009) High Sr/Y and La/Yb ratios: The meaning of the "adakitic signature". Lithos 112, 556-574.

Muir R.J., Weaver S.D., Bradshaw J.D., Eby G.N., Evans J.A. (1995) Geochemistry of the Cretaceous Separation Point Batholith, New Zealand: granitoid magmas formed by melting of mafic lithosphere. Journal of the Geological Society of London 152, 689-701.

Nebel O., Münker C., Nebel-Jacobsen Y.J., Kleine T., Mezger K., Mortimer N. (2007) Hf-Nd-Pb isotope evidence from Permian arc rocks for the long-term presence of the Indian-Pacific mantle boundary in the SW Pacific. Earth and Planetary Science Letters 254, 377-392.

Omrani J., Agard P., Whitechurch H., Benoit M., Prouteau G., Jolivet L. (2008) Arc-magmatism and subduction history beneath the Zagros Mountains, Iran: a new report of adakites and geodynamic consequences, Lithos 106, 380-398.

Peacock S.M., Rushmer T., Thompson A.B. (1994) Partial melting of subducting oceanic crust. Earth and Planetary Science Letters 121, 227-244.

Peccerillo P. and Taylor S.R. (1976) Geochemical of Eocene calkalkaline volcanic rocks from the Kastamonu area, northern Turkey. Contribution to Mineralogy and Petrology 58, 63-81.

Petford N. and Atherton M. (1996) Na-rich partial melts from newly underplated basaltic crust: the Cordillera Blanca batholith, Peru. Journal of Petrology 37, 1491-1521.

Prouteau G., Scaillet B., Pichavant M., Maury R.C. (1999) Fluid-present melting of oceanic crust in subduction zones. Geology 27, 1111-1114.

Rapp R. and Watson E. (1995) Dehydration melting of metabasalt at 8-32 kbar: Implications for continental growth and crust-mantle recycling. Journal of Petrology 36, 891-931.

Rapp R.P., Shimizu N., Norman M.D., Applegate G.S. (1999) Reaction between slab-derived melts and peridotite in the mantle wedge: experimental constraints at 3-8 GPa. Chemical Geology 160, 335-356.

Rapp R.P., Watson E.B., Miller C.F. (1991) Partial melting of amphibolite/eclogite and the origin of Archean trondhjemites and tonalities. Precambrian Research 51, l-25.

Rapp R.P., Xiao L., Shimizu N. (2002) Experimental constraints on the origin of potassium-rich adakite in east China. Acta Petrologica Sinica 18, 293-311.

Rollinson H. and Martin H. (2005) Geodynamic controls on adakite, TTG and sanukitoid genesis: implications for models of crust formation. Introduction to the Special Issue, Lithos 79, ix-xii.

Sajona F.G., Maury R.C., Pubellier M., Leterrier J., Bellon H., Cotten J. (2000) Magmatic source enrichment by slab-derived melts in a young post-collision setting, central Mindanao (Philippines). Lithos 54, 173-206.

Schroder J.W. (1944) Essai sur la structure de I'Iran. Eclogae Geologique Helvetique 37, 37-81.

Sen C. and Dunn T. (1994) Dehydration melting of a basaltic composition amphibolite at 1.5 and 2.0 GPa: implications for the origin of adakites. Contributions to Mineralogy and Petrology 117, 394-409.

Sen C. and Dunn T. (1994) Dehydration melting of a basaltic composition amphibolite at 1.5 and 2.0 GPa: implications for the origin of adakites. Contribution to Mineralogy and Petrology 117, 394-409.

Sengor A.M.C. (1990) A new modal for the late Paleozoic-Mesozoic tectonic evolution of Iran and implication for Oman. In: Roberson A.H.F., Srarle M.P., Ries A.C. (eds): The Geology and Tectonics of the Oman region. Geological Society of London Spec. Publ. 22, 278-281 (1990).

Shafaii Moghadam H., Whitechurch H., Rahgoshay M., Monsef I., (2009). Significance of Nain-Baft ophiolitic belt (Iran): Short-lived, transtensional Cretaceous back-arc oceanic basins over the Tethyan subduction zone. C.R. Geoscience 341, 1016-1028.

Skjerlie K.P. and Patino-Douce A.E. (2002) The fluid-absent partial melting of a zoisite-bearing quartz eclogite from 1.0 to 3.2 GPa: implications for melting in thickened continental crust and for subduction-zone processes. Journal of Petrology 43, 291-314.

Stern C.R. and Kilian R. (1996) Role of the subducted slab, mantle wedge and continental crust in the generation of adakites from the Andean Austral Volcanic Zone: Contributions to Mineralogy and Petrology 123, 263-281.

Stocklin J., (1968) Structural history and tectonics of Iran, a review, American Association Geological Bulletin 52, 1229-1258.

Stoneley R. The geology of the Kuh-e Dalneshin area of Southern Iran, and its bearing on the evolution of Southern Tethys, Geological Society, London, Special Publications 138, 509-526.

Sun S.S. and Mc Donough W.F. (1989) Chemical and isotopic systematics of oceanic basalts: implications for mantle composition and processes. In: Saunders A.D. and Norry M.J. (eds): Magmatism in the Ocean Basins. Geological Society Special Publication 42, 313-345.

Thompson R.N. (1982) British Tertiary volcanic province. Scottish Journal of Geology 18, 49-107.

Wang Q., McDermott F., Xu J.F., Bellon H., Zhu Y.T. (2005) Cenozoic K-rich adakitic volcanic rocks in the Hohxil area, northern Tibet: lower-crustal melting in an intracontinental setting. Geology 33, 465-468.

Winchester J.A. and Floyd P.A. (1977) Geochemical discrimination of different magma series and their differentiation products using immobile elements. Chemical Geology 20, 325-343.

Wood D.A. (1980) The application of a Th-Hf-Ta diagram to probiems of tectonomagmatic classification and to establishing the nature of crustal contamination of basaltic lavas of the

british Tertiary volcanic province. Earth and Planetary of Science Letters 50, 11-30.
Woodhead J.D., Hergt J.M., Davidson J.P., Eggins S.M. (2001) Hafnium isotope evidence for conservative element mobility during subduction zone processes. Earth and Planetary Science Letters 192, 331-346.
Xiong X.L., Li X.H., Xu J.F., Li W.X., Zhao Z.H., Wang Q., Chen X.M. (2003) Extremely high-Na adakite-like magmas derived from alkali-rich basaltic underplate: the Late Cretaceous Zhantang andesites in the Huichang Basin, SE China. Geochemical Journal 37, 233-252.
Xu J.F., Shinjio R., Defant M.J., Wang Q., Rapp R.P. (2002) Origin of Mesozoic adakitic intrusive rocks in the Ningzhen area of east China: partial melting of delaminated lower continental crust?. Geology 12, 1111-1114.
Zheng Y., Hou Z., Gong Y., Liang W., Sun Q., Zhang S., Fu Q., Huang K., Li Q., Li W. (2014) Petrogenesis of Cretaceous adakite-like intrusions of the Gangdese Plutonic Belt, southern Tibet: Implications for mid-ocean ridge subduction and crustal growth. Lithos (190-191), 240-263.